Heterogeneous Cosmological Phase Transition:

Seeded by Domain Walls and Junctions

Yiming Yang
University of Wisconsin-Madison

2026.01.29

Work with Yang Bai and Yifu Xu, 2512.10917

Content

1. Background
2. Heterogeneous phase transition
3. Heterogeneous cosmological PT
4. Example: $\mathbb{Z}_3$ potential

Background

- Cosmological first-order phase transition is related to many topics: electroweak baryogenesis, gravitational wave, etc.
- FOPT is described by **tunneling effect**[1]. The thermal tunneling rate $\gamma \propto e^{S_3/T}$, where S_3 is the **bouncing action**.
- The bouncing action corresponds to the instanton solution shaped as true vacuum **bubble**. It is a **saddle point** of action, through which the false vacuum transits into true vacuum in the field space.
- Critical action of **spherical** bubble (thin wall limit) is $S_{3,c}^{\text{homo}} \approx \frac{16\,\pi\,\sigma_{\text{B}}^3}{3\,\Delta V^2}$.
- In high-energy literature, only homogeneous PT is well-known, but actually, the defect-induced PT (or so-called **"heterogeneous"**) are richer and more important in condensed matter! [2]
- There are recent interests in defect-seeded PT (topological or not) for high energy! [3]

[1] S. R. Coleman, Phys. Rev. D **15** (1977), 2929-2936.
[2] D. Turnbull, Journal of Applied Physics **21** (10, 1950) 1022–1028.
[3] S. Blasi and A. Mariotti, Phys. Rev. Lett. **129** (2022) no.26, 261303 [arXiv:2203.16450]. S. Blasi and A. Mariotti, SciPost Phys. **18** (2025) no.1, 016 [arXiv:2405.08060].

Bubble on domain wall

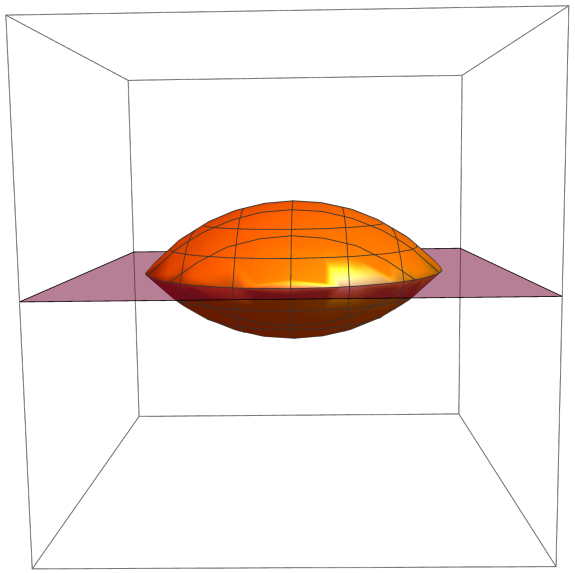

- If the bubble of FOPT happens at domain wall, we should expect: (i) locally the bubble is still spherical–so **spherical cap**; (ii) tension balance at boundary — from extremizing the action

$$S_3^{\rm W} = \mathcal{A}_{\rm surf.}\sigma_{\rm B} - \mathcal{V}\Delta V - \mathcal{A}_{\rm hole@DW}\sigma_{\rm DW}, \qquad (1)$$

where $\sigma_{\rm B}$ is surface tension of bubble, ΔV is potential difference of true and false vacuum, and $\sigma_{\rm DW}$ is tension of domain wall. The tension balance if from **Young equation**

contact angle

$$\sigma_{\rm DW} = 2\,\sigma_{\rm B}\,\cos\theta\,. \qquad (2)$$

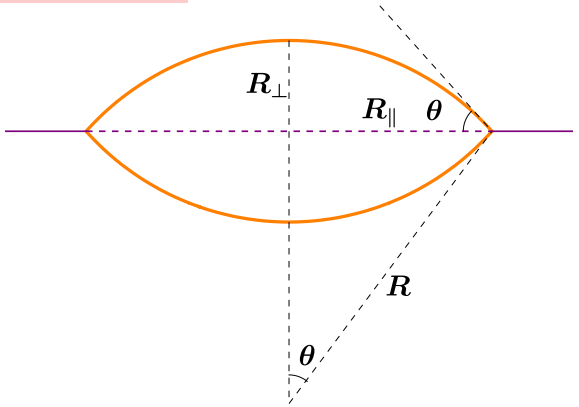

- The critical action for bubble on **domain wall**

$$S_{3,c}^{\rm W} = \frac{16\,\pi\,\sigma_{\rm B}^3}{3\,\Delta V^2}\,(1-\cos\theta)^2\left(1+\frac{\cos\theta}{2}\right)\,. \qquad (3)$$

Bubble on domain wall junction

- The critical action for bubble on **domain wall junction** at three walls (Y-type junction) with the same tension

$$S_{3,c}^{Y-\mathrm{J}} = \frac{8\,\sigma_{\mathrm{B}}^3}{3\,\Delta V^2}\left[\cos^2\theta\sqrt{3-4\cos^2\theta}\right. \tag{4}$$

$$\left. +\,3\cos\theta(\cos^2\theta-3)\arctan\left(\sqrt{\frac{3}{\cos^2\theta}-4}\right)+6\arctan\left(\sqrt{3-4\cos^2\theta}\right)\right],$$

  for $0 \le \cos\theta \le \sqrt{3}/2$. Note that the tension of junction is ignored.
- Similar things can be derived for other types of junctions.

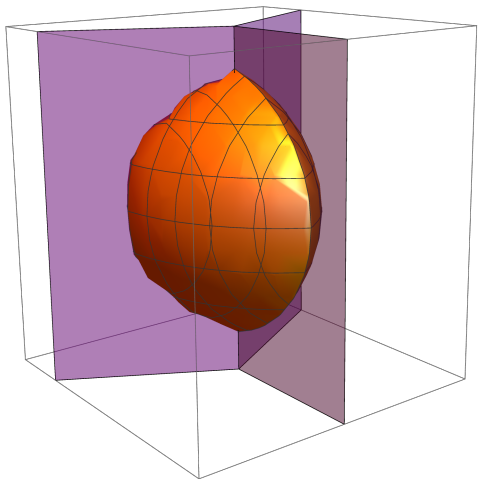

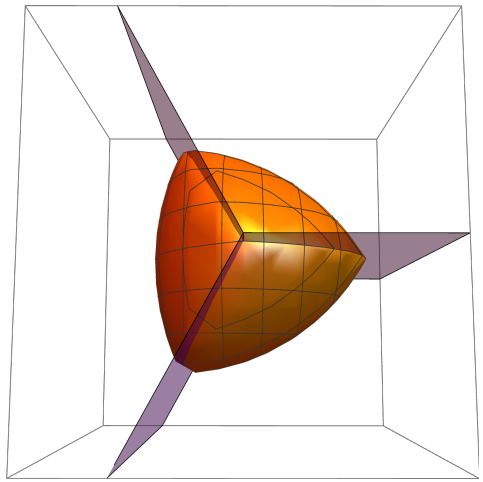

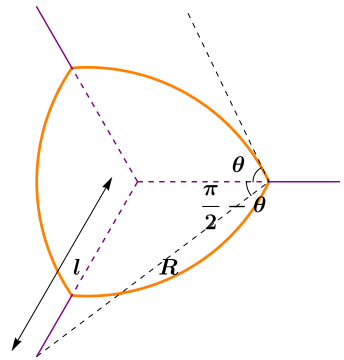

Heterogeneous phase transition: comment

- The critical radius is the same for all kinds of bubbles, as the homogeneous one, $R_c = 2\sigma_{\rm B}/\Delta V$: the action is extremized locally.
- The reduction factor of critical action is from the reduction of bubble **volume**.
- When the critical bubble expanses later (PT happens), the contact angle remains the same: the action has local minimum along $\cos\theta$.
- The criteria when the defect-induced PT is more important is determined by $\cos\theta = \sigma_{\rm DW}/2\sigma_{\rm B}$.

$\approx 3/4$

$\approx 2/4$, see next part

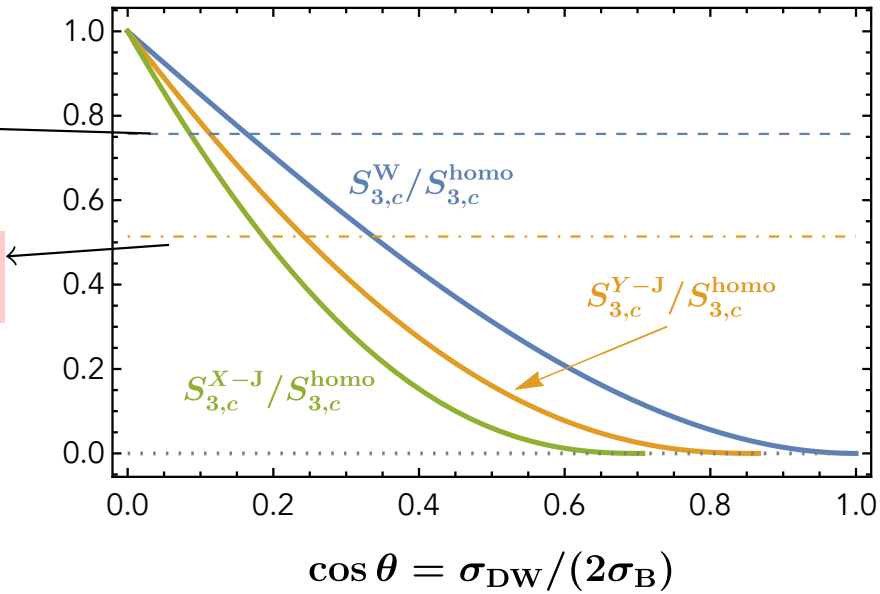

Decay rate

- The decay rate of the false vacuum per unit of volume in space is

$$\gamma = \frac{\Gamma}{V} = \frac{\xi\,\gamma_k\,V_k}{V}\,, \tag{5}$$

  where V is a large 3d spatial volume; ξ is the number of impurities in V. For homogeneous $\xi\,V_k/V = 1$; for scaling region of defects a fixed value.

- γ_k is the decay rate per k-dimensional volume (For DW, $k = 2$; for DWJ or string $k = 1$)

$$\gamma_k \approx T^{1+k}\left[\frac{B_k(T)}{2\pi}\right]^{3/2}\exp\left[-B_k(T)\right]\ ,\ \text{with}\quad B_k(T) \equiv S_3^{(k)}/T\ . \tag{6}$$

Nucleation temperature

- Take the starting point of PT is one bubble in each Hubble patch, and

$$\mathcal{N} = \xi \int_{t_c}^{t_n} \mathrm{d}t \, \frac{\gamma_k}{H^k} = \xi \int_{T_n}^{T_c} \frac{\mathrm{d}T}{T} \frac{\gamma_k}{H^{1+k}}. \tag{7}$$

With $\mathcal{N} \approx 1$, we call it **nucleation temperature** the reason of the lines in pervious plot

$$B_k(T_n) \approx (1+k) \log\left(\frac{T_n}{H(T_n)}\right) + \log \xi + 4.1 \ . \tag{8}$$

- For radiation-dominated universe, homogeneous $B_3(T_n) = 144$; DW-induced $B_2(T_n) = 109$; DWJ-induced $B_1(T_n) = 74$.
- The finish of PT is labeled by **percolation temperature**, which consider how much ratio of the space can be covered by true vacuum. (i) percolation on the defect $T_p^{(k)}$; (ii) percolation for the whole space T_p, different for dilute DW network, with $T_p \approx T_p^{(k)} \left(1 - v_{\mathrm{sh}}^{-1} \, \xi^{-1}\right)$.

$\mathbb{Z}_3$ potential setup

- Consider a model with one real scalar field ϕ and one complex scalar field S charged under a $\mathbb{Z}_3$ symmetry, and a two-step PT. The global minimum of potential for VEV of $(\langle S\rangle, \langle\phi\rangle)$, when temperature deceases is:

$$(0,0) \to (v_S, 0) \to (0, v_\phi) \tag{9}$$

  The first step spontaneously breaks the $\mathbb{Z}_n$ symmetry and generates DWs and DWJs. The second step is FOPT: At T_c, the global minimum is along the ϕ, and thermal tunneling will take $(v_S, 0) \to (0, v_\phi)$.
- The $\mathbb{Z}_2$ with ϕ being EW Higgs is well-studied.[1]
- In high temperature limit, the $\mathbb{Z}_3$-symmetric S and ϕ potential is

$$\begin{aligned} V(S,\phi,T) = &-\left(\mu_0^2 - c_1 T^2\right) S^* S + \lambda_1 \left(S^* S\right)^2 - \lambda_2\, \mu_0 \left(S^3 + S^{*3}\right) \\ &- \frac{m^2 - c_2 T^2}{2}\, \phi^2 + \frac{\eta_3\, m}{3}\, \phi^3 + \frac{\eta_4}{4}\, \phi^4 + \kappa\, \phi^2\, S^* S\,, \end{aligned} \tag{10}$$

  with $c_1 = (4\lambda_1 + \kappa)/12$ and $c_2 = (3\eta_4 + 2\kappa)/12$.

[1] S. Blasi and A. Mariotti, Phys. Rev. Lett. **129** (2022) no.26, 261303 [arXiv:2203.16450]. P. Agrawal, S. Blasi, A. Mariotti and M. Nee, JHEP **06** (2024), 089 [arXiv:2312.06749].

Methods to find bounce action

- Write $S = (s + i\,a)/\sqrt{2}$ [1], and $\chi \equiv 3\lambda_2/\sqrt{8\lambda_1}$.
- Three methods to derive the bounce action S_3^c .
- **Thin wall limit**: As the first part;
- **tanh-profile**: The transition of the field profiles are always like tanh shape, so we use variation method on some parameters in tanh profile

$$\varphi(r) = \frac{v_{\varphi,\mathrm{F}} - v_{\varphi,\mathrm{T}}}{2}\left(1 + \tanh\left[\frac{r - r_\varphi}{\sqrt{2}\,d_\varphi}\right]\right) + v_{\varphi,\mathrm{T}}\,, \tag{11}$$

  where r is the radial distance from the center of the bubble, d_φ is the wall thickness, and r_φ is the transition radius. For practical reason, we will fix some of r_φ or d_φ are the same;
- **Mountain pass theorem (MPT) algorithm**: Developed in literature[2] and gives numerical solution for bouncing profile as saddle point of action.

[1] Define the dimensionless fields and parameters $\bar{s} = \sqrt{\lambda_1}s/\mu_0$, $\bar{a} = \sqrt{\lambda_1}a/\mu_0$, $\bar{\phi} = \sqrt{\lambda_1}\phi/\mu_0$, $\bar{T} = \sqrt{\lambda_1}T/\mu_0$, $\bar{\eta}_3 = \eta_3\, m/(\mu_0\sqrt{\lambda_1})$, $\bar{\eta}_4 = \eta_4/\lambda_1$, $\bar{\kappa} = \kappa/\lambda_1$, and normalize the coordinates as $\bar{z} = \mu_0\, z$ and $\bar{\rho} = \mu_0\, \rho$.

[2] P. Agrawal and M. Nee, SciPost Phys. **13** (2022) no.3, 049 [arXiv:2202.11102].

Results of profiles

- Choose a benchmark point $\chi = 0.1$, $m/\mu_0 = 1.2$, $\lambda_1 = 1$, $\bar{\kappa} = 7.5$, $\bar{\eta}_4 = 0.6$, and $\eta_3 = 0$, with $T = 0.92\,T_c$ where $T_c = 0.974\,\mu_0$.
- The solution solved from MPT for **DW** is

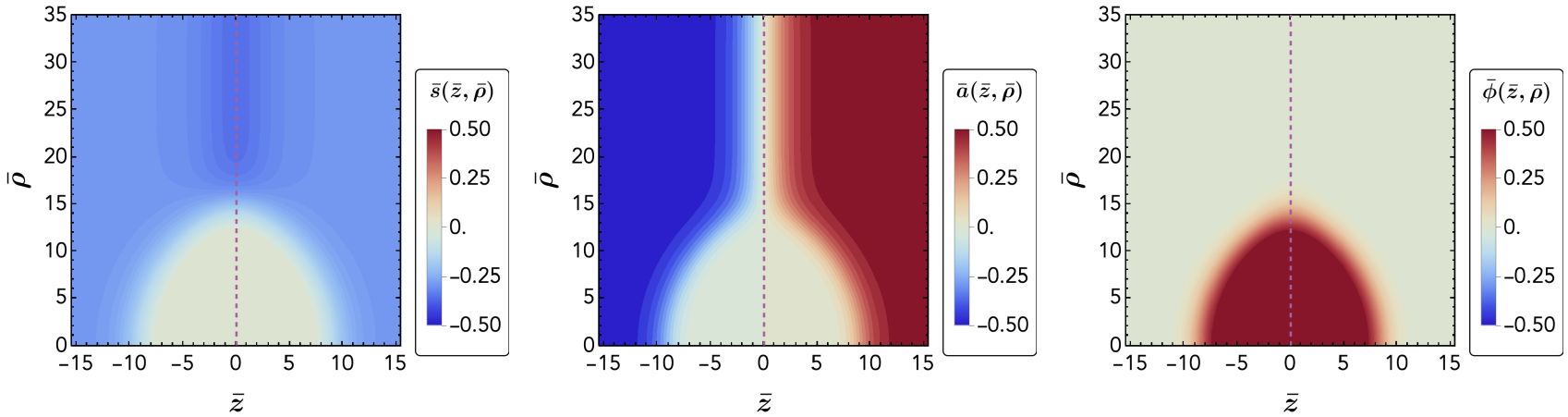

- Although for $\mathbb{Z}_3$ potential, the middle point in field space is local maximum, unlike $\mathbb{Z}_2$ which is the would-be true vacuum 0, the DW-induced one is still possible, and faster!

Results of profiles

- For the same benchmark point. The tanh-profile method for **DWJ** is as follows (because MPT is hard to solve for 3d problem)

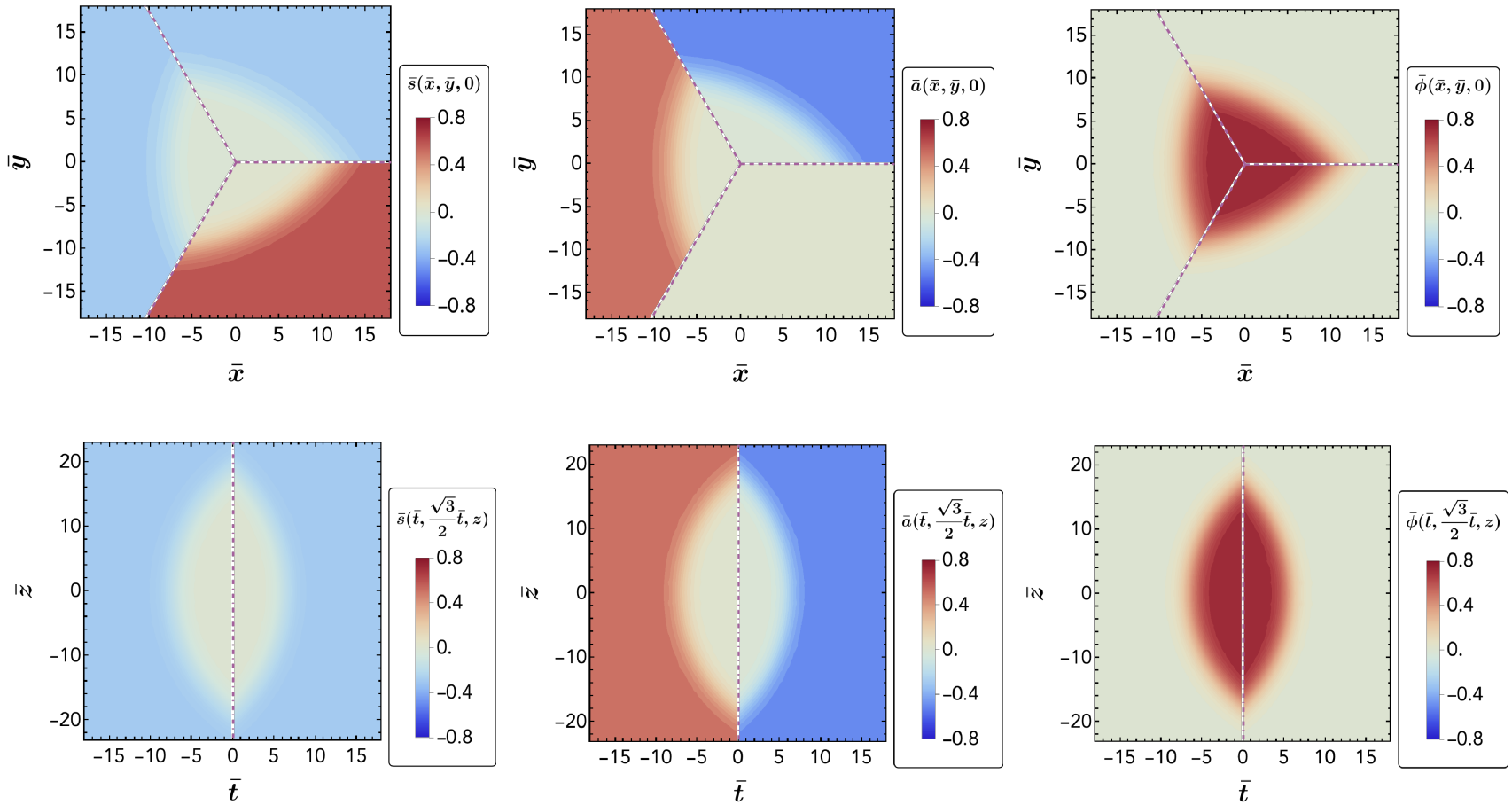

- The DW and DWJ outside the bubble is not shown in this method.

Results of actions

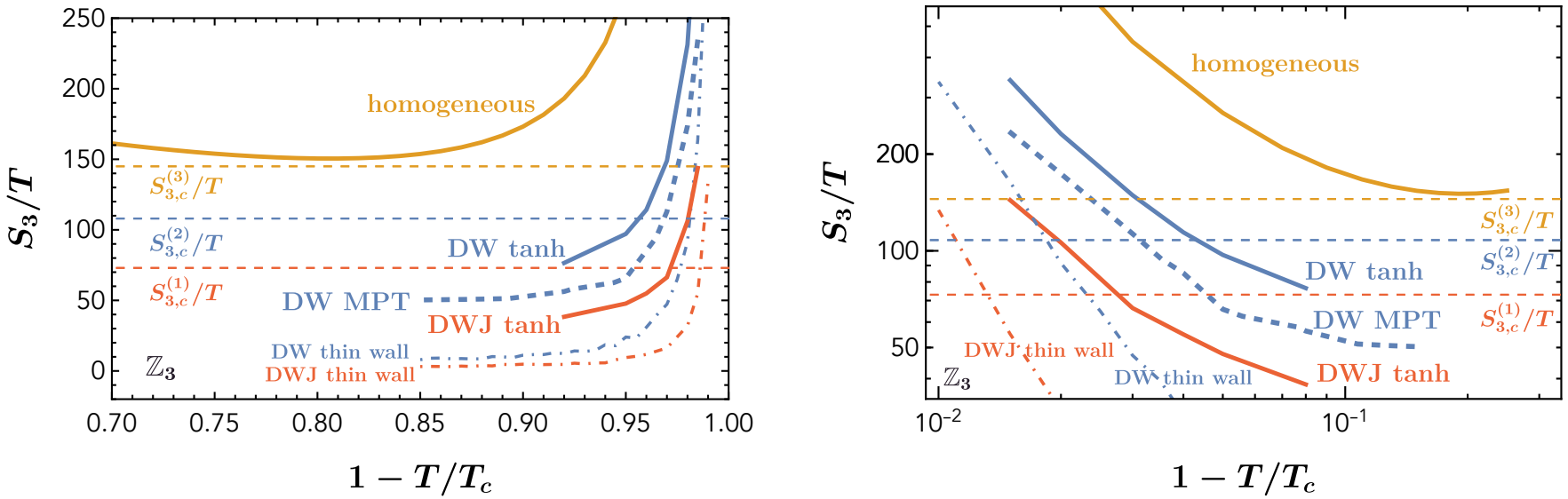

- For this benchmark, the homogeneous PT is not possible to happen.
- Using the tanh-profile results, the nucleation temperatures are $T_n^{(2)} = 0.957\,T_c$ for DW-seeded nucleation and $T_n^{(1)} = 0.973\,T_c$ for DWJ-seeded nucleation, clearly demonstrating that junction-seeded nucleation is more efficient!

Conclusion

- The heterogeneous PT is more efficient than homogeneous PT usually.
- The critical action and its dynamics is characterized by the contact angle $\cos\theta = \sigma_{\mathrm{DW}}/2\sigma_{\mathrm{B}}$.
- Tanh-profile can help to model the bubble better than thin wall limit.
- The cosmological phenomenological sequences will be interesting to study.

Thanks!

Backup

Bubble on Y-type junction with arbitrary angle

- The critical action for bubble on Y-type junction with two same tension σ_1 (with angle θ_1) and one different tension σ_2 (with θ_2) is

$$S_{3,c}^{Y-\mathrm{J,II}} = \frac{4\sigma_{\mathrm{B}}^3}{\Delta V^2}\left\{\frac{\cos^2\theta_1}{3\sin^2\frac{\alpha}{2}}(2\sin\alpha-\sin 2\alpha)\sqrt{1-\frac{\cos^2\theta_1}{\sin^2\frac{\alpha}{2}}}\right. \tag{12}$$

$$-\left[4\left(\cos\theta_1-\frac{1}{3}\cos^3\theta_1\right)\arctan\left(\frac{\sqrt{\sin^2\frac{\alpha}{2}-\cos^2\theta_1}}{\cos\theta_1\cos\frac{\alpha}{2}}\right)-\frac{8}{3}\arctan\left(\frac{\sqrt{\sin^2\frac{\alpha}{2}-\cos^2\theta_1}}{\cos\frac{\alpha}{2}}\right)\right.$$

$$\left.\left.+2\left(\cos\theta_2-\frac{1}{3}\cos^3\theta_2\right)\arctan\left(\frac{\sqrt{\sin^2\alpha-\cos^2\theta_2}}{\cos\theta_2|\cos\alpha|}\right)-\frac{4}{3}\arctan\left(\frac{\sqrt{\sin^2\alpha-\cos^2\theta_2}}{\cos\theta_2|\cos\alpha|}\right)\right]\right\},$$

  for $\alpha\in(\frac{\pi}{2},\pi]$.

- Note that we have already used Young's equation to simplify the calculation by expressing

$$\frac{\sigma_1}{2\sigma_{\mathrm{B}}}=\cos\theta_1\,,\quad \frac{\sigma_2}{2\sigma_{\mathrm{B}}}=\cos\theta_2\,,\quad \frac{\sigma_2}{2\sigma_1}=\cos\frac{\alpha}{2}\,, \tag{13}$$

- When $\alpha=\frac{\pi}{2}$, the terms involving arctan of θ_2 should be interpreted as approaching $\frac{\pi}{2}$. When $\alpha\in[0,\frac{\pi}{2})$, one has an addition term, $(2/3)(\pi-2\alpha)\sqrt{1-\cos^2\theta_2/\sin^2\alpha}\,(2+\cos^2\theta_2/\sin^2\alpha)$, inside the curly braces.

Bubble on X-type junction with angle $\pi/2$

- For example in $\mathbb{Z}_4$ there are two types of X-junction, but the non-adjacent one is always unstable and will split into two Y-type junction, and the adjacent one is stable when $\sigma_2 > \sqrt{2}\sigma_1$.
- The critical action is

$$S_{3,c}^{X-\mathrm{J}} = \frac{32\,\sigma_{\mathrm{B}}^3}{3\,\Delta V^2}\left[\cos^2\theta\sqrt{1-2\cos^2\theta}\right. \tag{14}$$
$$\left. + \cos\theta\,(\cos^2\theta - 3)\arctan\left(\sqrt{\frac{1}{\cos^2\theta}-2}\right) + 2\arctan\left(\sqrt{1-2\cos^2\theta}\right)\right] .$$

- More complicated DWJ may be unstable, see the reference.[1]

[1] P. Pina Avelino, C. J. A. P. Martins, J. Menezes, R. Menezes and J. C. R. E. Oliveira, Phys. Rev. D **73** (2006), 123519 [arXiv:astro-ph/0602540].

Percolation temperature

- First percolation is the percolation on the defect. The probability of remaining in the false vacuum $p_k(t)$ in k dimensions is

$$p_k(t) = \exp\left[-\frac{2}{k}\frac{\pi^{k/2}}{\Gamma\left(\frac{k}{2}\right)}\int_{t_c}^{t} \mathrm{d}t'\, v_{\mathrm{sh}}^k\,(t-t')^k\,\gamma_k(t')\right]. \tag{15}$$

  and we expect $p_k(t_p^{(k)}) = 0.32$.

- If the domain walls are dilute, $t_p^{(k)}$ is not enough to finish the PT in 3d, we can expect the planar bubbles (merged from bubbles on DW) or cylinder bubbles (from DWJ) expanse to cover the whole space, so there will be a true percolation time t_p.

Percolation temperature

- The criteria ξ_0 can be derived from comparing separation distance between two domain walls, $\xi^{-1}/H(T_p^{(k)})$, and bubble radius $R_p^{(k)} \approx N_{\rm nuc}^{1/k}/H(T_p^{(k)})$, with number of bubbles

$$N_{\rm nuc} \approx \frac{1}{[H(T_p^{(k)})]^k} \int_{t_c}^{t} {\rm d}t' \gamma_k(t') p_k(t') \approx \frac{1}{A_k} \left(\frac{\beta}{H(T_p^{(k)})} \right)^k , \tag{16}$$

with $A_k \equiv 2\pi^{k/2}\Gamma(k+1) v_{\rm sh}^k/(k\Gamma\left(\frac{k}{2}\right))$ and $\beta \equiv TH\, {\rm d}B_k/{\rm d}T|_{T=T_p^{(k)}}$. Then

$$\xi_0 = \frac{2\, B_k\, T_p^{(k)}}{T_c - T_p^{(k)}}. \tag{17}$$

- The separation distance between impurities is (radiation dominated) $L(t) \approx \xi^{-1}[H(T_p^{(k)})]^{-1}(t/t_p^{(k)})^{1/2}$ from scaling, while the grown bubble radius is $R(t) \approx R(t_p^{(k)}) + v_{\rm sh}\,(t - t_p^{(k)})$. Requiring $R(t) = L(t)$, we have

$$T_p \approx T_p^{(k)} \left(1 - v_{\rm sh}^{-1}\, \xi^{-1}\right) . \tag{18}$$

$\mathbb{Z}_2$ potential example: setup

- For two real scalar fields ϕ and S with a $\mathbb{Z}_2$ symmetric S field

$$V_0(\phi, S) = -\frac{\mu_S^2}{2} S^2 + \frac{\lambda}{4} S^4 - \frac{\mu_\phi^2}{2} \phi^2 + \frac{\eta}{4} \phi^4 + \frac{\kappa}{2} \phi^2 S^2 \,. \tag{19}$$

- The finite-temperature potential is

$$V_T = \frac{T^4}{2\pi^2} \left[J_B\left(\frac{M_S^2}{T^2}\right) + J_B\left(\frac{M_\phi^2}{T^2}\right) \right] , \tag{20}$$

where $J_B(y^2) = \int_0^\infty \mathrm{d}x\, x^2 \log[1 - \exp(-\sqrt{x^2 + y^2})]$, $M_S^2 = -\mu_S^2 + 3\lambda\, S^2 + \kappa\, \phi^2$ and $M_\phi^2 = -\mu_h^2 + 3\eta\, \phi^2 + \kappa\, S^2$. The leading two terms of the high-temperature expansion of $J_B(y^2) \approx -\frac{\pi^4}{45} + \frac{\pi^2}{12} y^2$.

- The total effective potential

$$V(\phi, S, T) \approx \frac{c_S T^2 - \mu_S^2}{2} S^2 + \frac{\lambda}{4} S^4 + \frac{c_\phi T^2 - \mu_\phi^2}{2} \phi^2 + \frac{\eta}{4} \phi^4 + \frac{\kappa}{2} \phi^2 S^2 \,. \tag{21}$$

Here $c_\phi \equiv (3\eta + \kappa)/12$ and $c_S \equiv (3\lambda + \kappa)/12$. [1]

[1] If ϕ is the radial mode of the SM Higgs, $c_\phi = (2m_W^2 + m_Z^2 + m_h^2 + 2m_t^2)/(4v_{\rm EW}^2) + \kappa/12$, $c_S = (3\lambda + 4\kappa)/12$ with $v_{\rm EW} = 246$ GeV, $\mu_\phi = 88$ GeV and $\eta = 0.129$.

$\mathbb{Z}_2$ potential example: results

- For EW Higgs, and $\kappa = 1.3$, $\lambda = 1.6$, $\mu_S = 127$ GeV

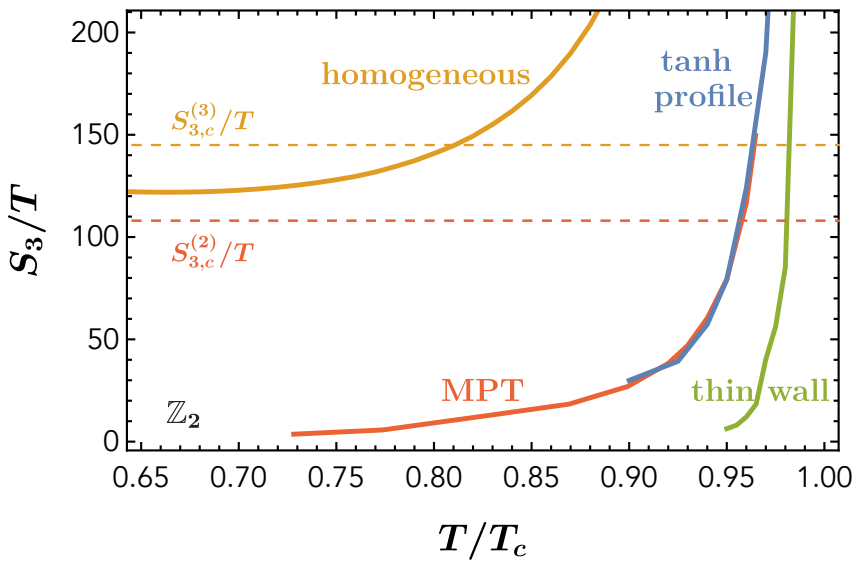

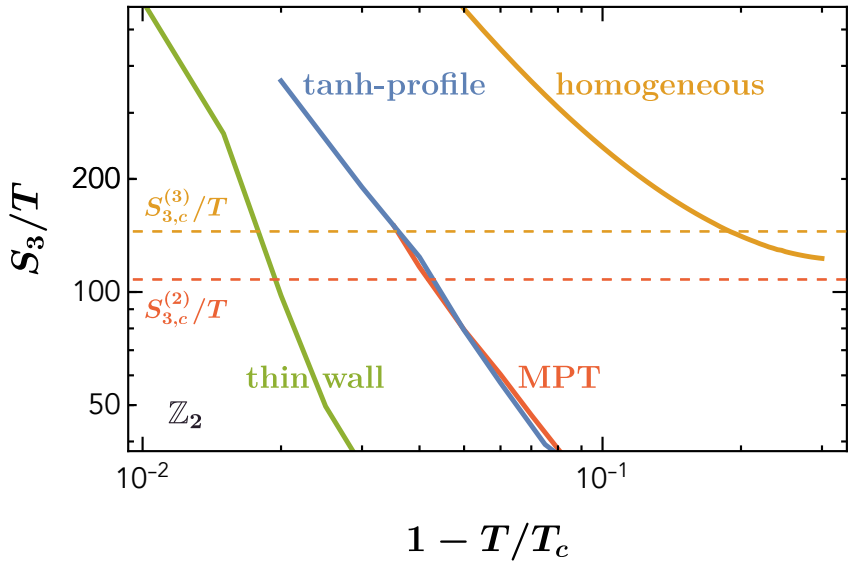

- MPT result is the same as reference[1].
- tanh-profile gives very good agreement of the numerical "true" results! If we can employ the variation method with more parameters in $\mathbb{Z}_3$, maybe we can reach better results!

[1] P. Agrawal, S. Blasi, A. Mariotti and M. Nee, JHEP **06** (2024), 089 [arXiv:2312.06749].

$\mathbb{Z}_3$ potential: high temperature limit

- For $\mathbb{Z}_n$ symmetric S, the renormalizable zero-temperature potential is

$$V(s,a,\phi,T=0) = -\frac{m^2}{2}\phi^2 + \frac{\eta_3\, m}{3}\phi^3 + \frac{\eta_4}{4}\phi^4 + \frac{\kappa}{2}\phi^2(s^2+a^2)$$
$$- \frac{\mu_0^2}{2}(s^2+a^2) + \frac{\lambda_1}{4}(s^2+a^2)^2 - \frac{\lambda_2\mu_0^{4-n}}{2^{(4-n)/2}} \sum_{l<(n-2)/2} (-1)^l\, C_n^{2l}\, s^{n-2l}\, a^{2l}\,. \qquad (22)$$

The temperature correction is also

$$V_T = \frac{T^4}{2\pi^2}\left[J_B\left(\frac{M_s^2}{T^2}\right) + J_B\left(\frac{M_a^2}{T^2}\right) + J_B\left(\frac{M_\phi^2}{T^2}\right)\right], \qquad (23)$$

where

$$M_s^2 = -\mu_0^2 + \lambda_1\,(3s^2+a^2) + \frac{\lambda_2\,\mu_0^{4-n}}{2^{(4-n)/2}}\, n(n-1)\sum(-1)^l C_{n-2}^{2l}\, s^{n-2l-2}\, a^{2l} + \kappa\,\phi^2\,,$$
$$M_a^2 = -\mu_0^2 + \lambda_1\,(3a^2+s^2) + \frac{\lambda_2\,\mu_0^{4-n}}{2^{(4-n)/2}}\, n(n-1)\sum(-1)^l\, C_{n-2}^{2l-2}\, s^{n-2l}\, a^{2l-2} + \kappa\,\phi^2\,,$$
$$M_\phi^2 = -m^2 + 2\eta_3\, m\,\phi + 3\eta_4\,\phi^2 + \kappa\,(s^2+a^2)\,. \qquad (24)$$

- Then we get the pervious results. For $n=3$, there is an additional correction to the term $\lambda_2\,\mu_0(S^3+S^{*3})$ in the high-temperature limit, which is small for perturbative couplings.

$\mathbb{Z}_3$ potential: numerical junction profile

- The junction profile can be solved numerically. E.g. The $\mathbb{Z}_3$ symmetric S at $T = 0$ and $\chi \equiv 3\lambda_2/\sqrt{8\lambda_1} = 0.1$, we have Y-type junction.

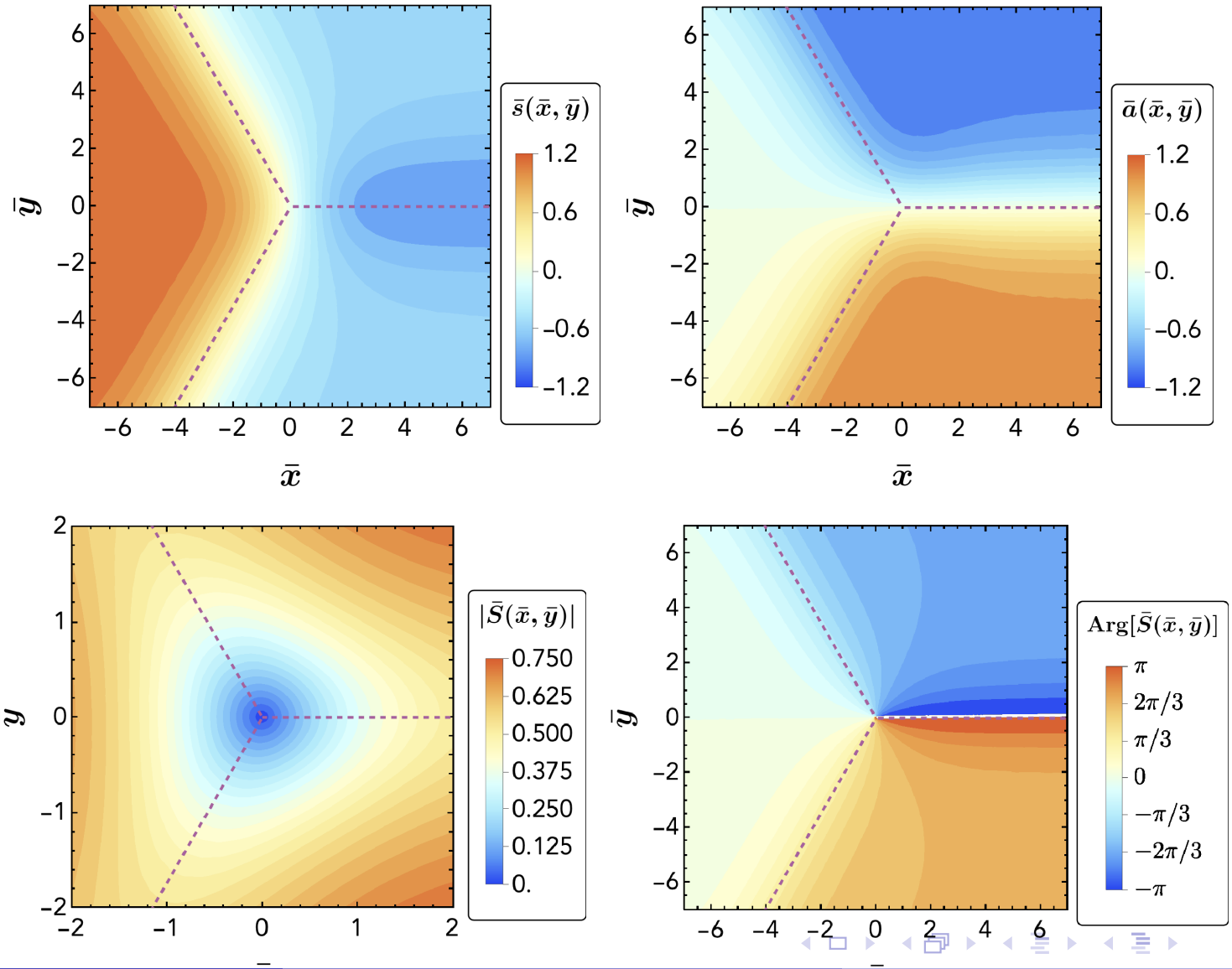

Constraint on $\sigma_{\rm DW}/\sigma_{\rm B}$ for the scalar field model

- In thin wall limit, one can show that $\sigma_{\rm DW} < 2\sigma_{\rm B}$.
- The bubble-wall tension is

$$\sigma_{\rm B} = \int_{R-\delta R}^{R+\delta R} {\rm d}r \left(\frac{1}{2} \sum_i \left[\frac{{\rm d}\varphi_i}{{\rm d}r} \right]^2 + \left[V(\phi_i) - V(\varphi_i^*) \right] \right) , \tag{25}$$

where φ_i^* is the release point on the true-vacuum side $V(\varphi_i^*) = V(\varphi_i^{\rm F})$. In thin wall limit, $\varphi_i^{\rm T} = \varphi_i^*$.

$$\langle S \rangle^{\rm F_1} = v_S(T)\, e^{2\pi i/3}$$
$$\langle S \rangle^{\rm F_2} = v_S(T)\, e^{4\pi i/3}$$

- We take φ_1 to be the field a and consider the bubble transiting from $\varphi_1(R-\delta R) = a^{\rm T}$ to $\varphi_1(R+\delta R) = a^{\rm F_1}$. With EoM

$$\sigma_{\rm B} = \int_{\varphi_1^{\rm T}=0}^{\varphi_1^{\rm F_1}} {\rm d}\varphi_1 \sqrt{\sum_{i=1}^{n} \left(\frac{{\rm d}\varphi_i}{{\rm d}\varphi_1} \right)^2} \sqrt{2\left[V(\varphi_i) - V(\varphi_i^{\rm T}) \right]} . \tag{26}$$

In order to compare $2\sigma_{\rm B}$ with $\sigma_{\rm DW}$, we add another path connecting T and $\rm F_2$.

$$2\,\sigma_{\rm B} = \int_0^{\varphi_1^{\rm F_1}} {\rm d}\varphi_1 \sqrt{\sum_{i=1}^{n} \left(\frac{{\rm d}\varphi_i^{\rm F_1}}{{\rm d}\varphi_1^{\rm F_1}} \right)^2} \sqrt{2[V(\varphi_i^{\rm F_1}) - V(\phi_i^{\rm T})]}$$
$$+ \int_0^{\varphi_1^{\rm F_2}} (-{\rm d}\varphi_1) \sqrt{\sum_{i=1}^{n} \left(\frac{{\rm d}\varphi_i^{\rm F_2}}{{\rm d}\varphi_1^{\rm F_2}} \right)^2} \sqrt{2[V(\varphi_i^{\rm F_2}) - V(\varphi_i^{\rm T})]} \tag{27}$$

Constraint on $\sigma_{\rm DW}/\sigma_{\rm B}$ for the scalar field model

- If we define the path connecting F_1 and F_2 by $\varphi_i^{\rm B} = \begin{cases} \varphi_i^{\mathrm{F}_2} & \varphi_1 \in [\varphi_1^{\mathrm{F}_2}, 0] \\ \varphi_i^{\mathrm{F}_1} & \varphi_1 \in [0, \varphi_1^{\mathrm{F}_1}] \end{cases}$, which corresponds to following the two sides of the triangle between F_1 and F_2 rather than the straight line connecting them. The tension is

$$2\sigma_{\rm B} = \int_{\varphi_1^{\mathrm{F}_2}}^{\varphi_1^{\mathrm{F}_1}} \mathrm{d}\varphi_1 \sqrt{\sum_{i=1}^{n} \left(\frac{\mathrm{d}\varphi_i^{\rm B}}{\mathrm{d}\varphi_1^{\rm B}}\right)^2} \sqrt{2[V(\varphi_i^{\rm B}) - V(\varphi_i^{\rm T})]}\,. \tag{28}$$

- Note that the domain-wall tension $\sigma_{\rm DW}$ can be written in exactly the same form as the right side, except that the fields follow the domain-wall trajectory $\varphi_i^{\rm DW}$. As long as the domain wall is stable, the path $\varphi_i^{\rm DW}$ corresponds to a local minimum of the one-dimensional action and therefore minimizes the tension. Consequently, one obtains $\sigma_{\rm DW} < 2\sigma_{\rm B}$.
- However, this does not rule out complete wetting, because the ratio $\sigma_{\rm DW}/2\sigma_{\rm B}$ appears only within the thin-wall approximation, e.g. the $SU(3)_c$ Polyakov-loop potential—the $\mathrm{T}-\mathrm{F}$ and $\mathrm{F}-\mathrm{F}$ wall thicknesses can be comparable to the size of the true vacuum.

Hessian operator

- The stability for both the vacuum solutions and the instanton solution is given by the Hessian operator of the Euclidean action. E.g.

$$I(\phi, S) = \int \mathrm{d}^D x \left[\frac{1}{2} \partial_\mu \phi \partial^\mu \phi + \frac{1}{2} \partial_\mu S \partial^\mu S + V(\phi, S) \right] . \tag{29}$$

- From the second order variation around the classical solution (ϕ_0, S_0) of EoM to $(\phi_0 + \delta\phi, , S_0 + \delta S)$ and obtain

$$\delta I(\phi, S) \supset \int \mathrm{d}^D x \frac{1}{2} \left[\begin{pmatrix} \delta\phi & \delta S \end{pmatrix} \hat{O}(\phi_0, S_0) \begin{pmatrix} \delta\phi \\ \delta S \end{pmatrix} \right] , \tag{30}$$

where the Hessian operator for this action

$$\hat{O}(\phi_0, S_0) = \begin{pmatrix} -\partial_\mu \partial^\mu + \frac{\partial^2 V}{\partial \phi^2} & \frac{\partial^2 V}{\partial \phi \, \partial S} \\ \frac{\partial^2 V}{\partial \phi \, \partial S} & -\partial_\mu \partial^\mu + \frac{\partial^2 V}{\partial S^2} \end{pmatrix} \Bigg|_{\phi=\phi_0 \,, \, S=S_0} . \tag{31}$$

- If $\hat{O}$ is semi–positive definite, the solution (ϕ_0, S_0) is a local minimum and corresponds to a vacuum.
- If negative eigenvalues exist, the solution is unstable and represents a saddle point.